Supporting Information

Manipulation of 2DEG at Double-doped High-entropy Heterointerfaces

Hang Yin, Ruishu Yang, Shuanhu Wang, Kexin Jin*

Shaanxi Key Laboratory of Condensed Matter Structures and Properties and MOE Key Laboratory of Materials Physics and Chemistry under Extraodinary Conditions, School of Physical Science and Technology, Northwestern Polytechnical University, Xi'an 710072, China.

Supplementary data section

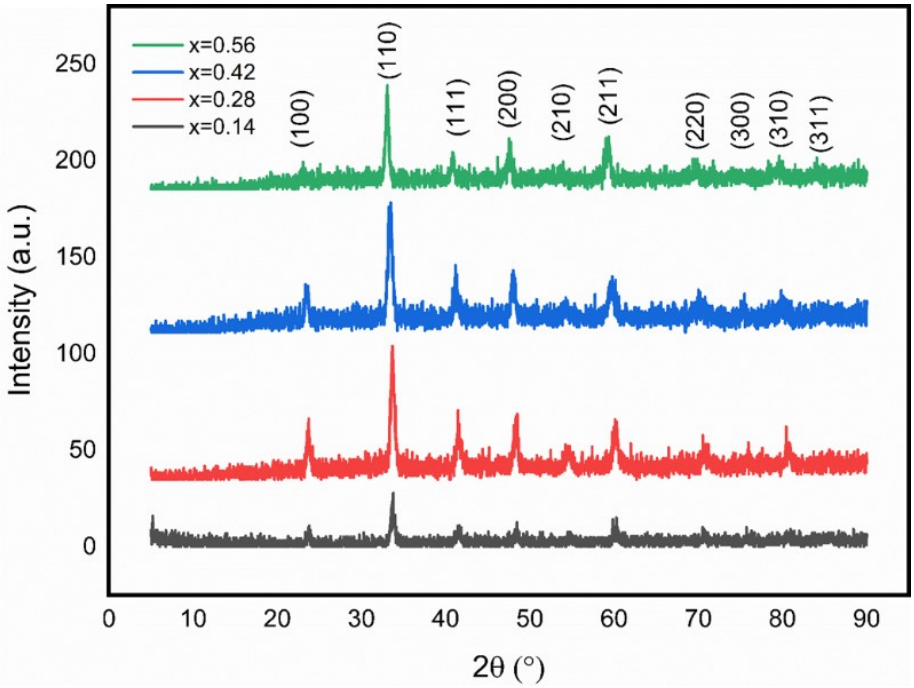

Figure S1. X-ray diffraction (XRD) result of different $Nd_{1-x}Sr_xAl_{1-x}Mn_xO_3$ (NSAMO) targets.

For four different targets, the peak position of their XRD results keeps almost the same although with little shift with the change of doping ratio x compared with standard PDF card of $NdAlO_3$ (NAO) (ICDD/JPCDS PDF-#29-0056). The cubic structure is maintained, and the calculated

tolerance factor (t) are as follows: 0.876(x=0.14), 0.877(x=0.28), 0.878(x=0.42), 0.883(x=0.56). These results confirms a stable crystalline structure after different level of doping.

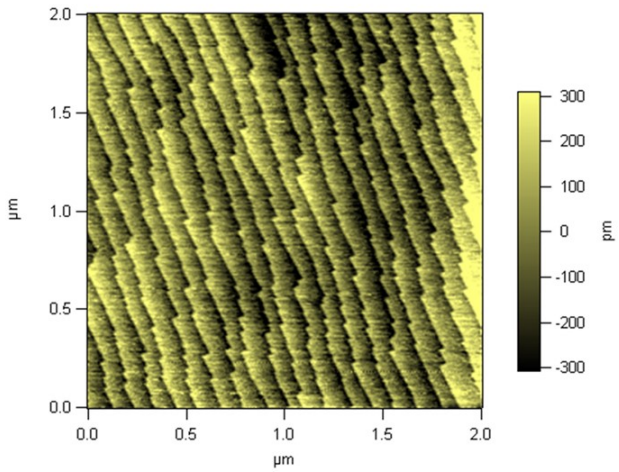

Figure S2. Atomic force microscope (AFM) image of pretreated (001) $SrTiO_3$ (STO) substrate.

Before the film growth, the (001) face STO substrate is pre-treated to get TiO_2 terminated surface. The flat surface and regular terraces are obtained, and its surface root-mean-square (RMS) roughness value are only 134.913 pm.

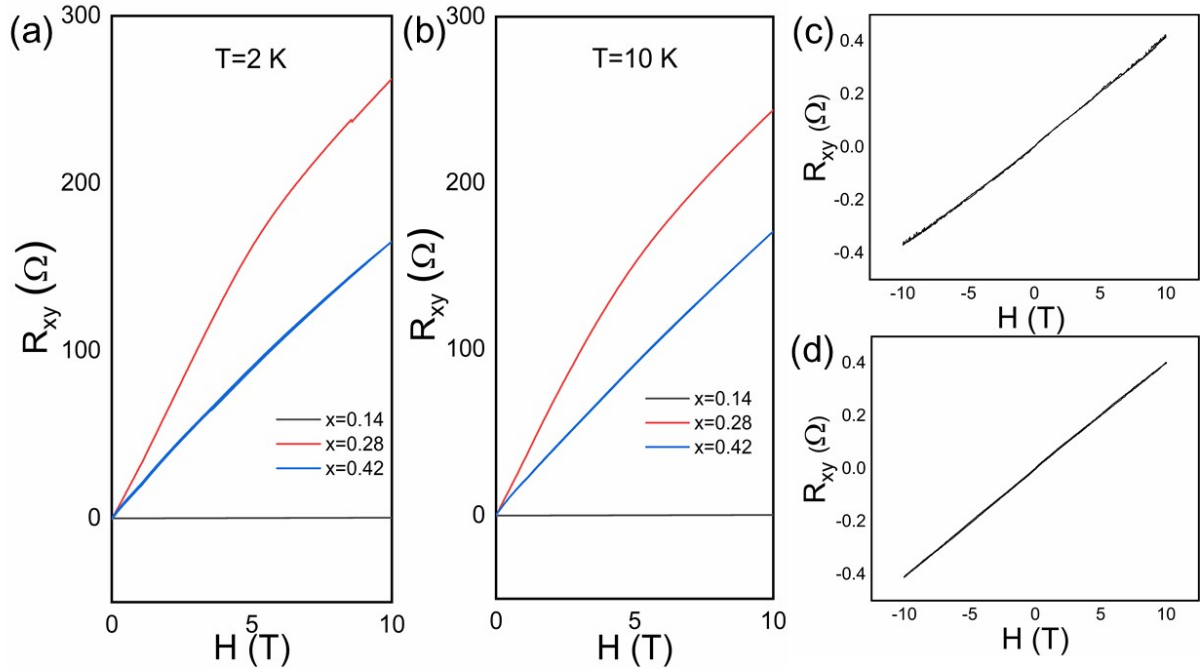

Figure S3. Hall resistance as a function of magnetic field of the sample with x=0.14-0.42, the film thickness are all 30 nm. (a) At 2 K. (b) at 10 K. Magnified Hall resistance results of x=0.14 samples shown in Fig. S3a and S3b. (c) At 2 K. (d) At 10 K.

At 2 K and 10 K, Hall resistance with respect to magnetic field (R_{xy}-H) results for x=0.14, 0.28 and 0.42 are shown in Fig. S3, the film thickness are all 30 nm. When x=0.14, the R_{xy}-H is linear because of solely d_{xy} conduction. When x=0.28 and 0.42, the samples both show unlinear R_{xy}-H curves. The former can be attributed to abnormal Hall effect (AHE), while the latter one can be the results of AHE and dual-channel carriers.

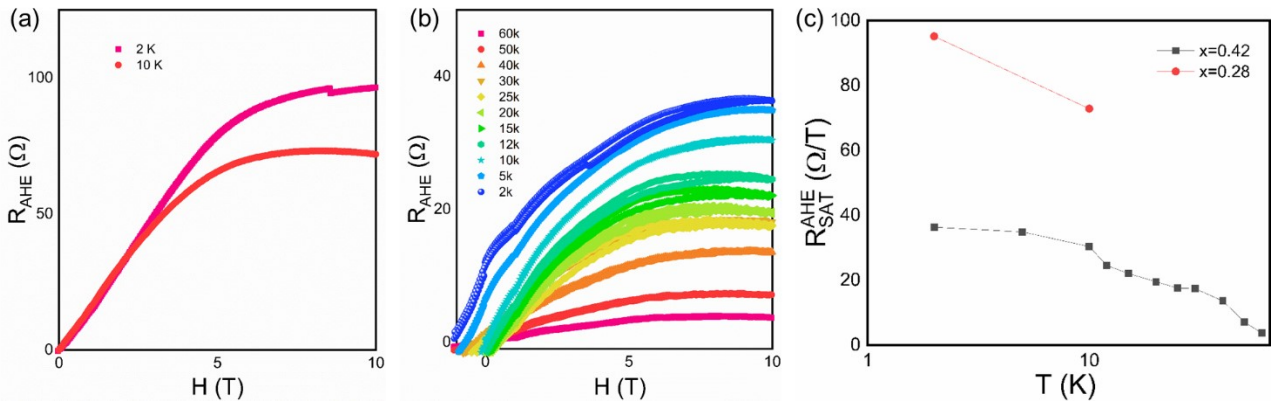

Figure S4. Abnormal Hall resistance (R_{AHE}) extracted from nonlinear R_{xy}-H results for (a) x=0.28 and (b) x=0.42. (c) Saturation abnormal Hall resistance as a function of temperature (R_{AHE}-T) extracted from Fig. S4(a) and (b).

The R_{AHE} results for x=0.28 and 0.42 samples with respect to magnetic field are extracted from nonlinear R_{xy}-H results after their linear part is deduced. The step-like feature is obvious, while the most dramatic change happens below 5 T. After 5 T, the results tend to become saturated.

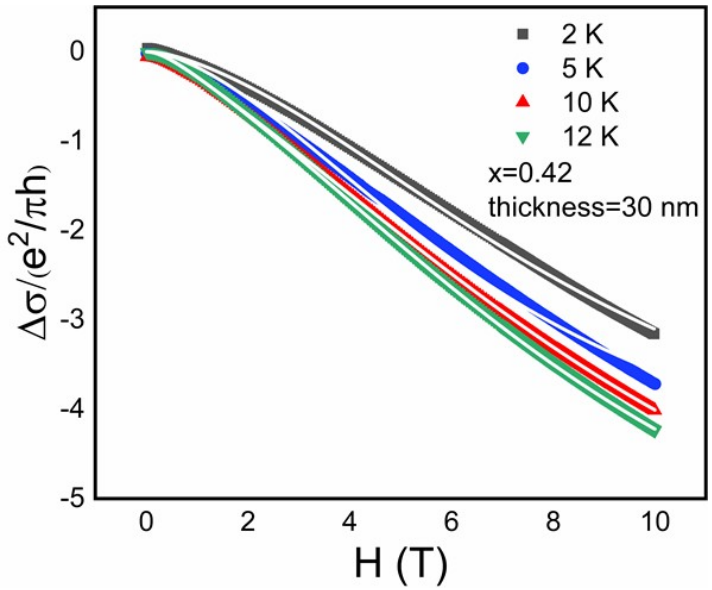

Figure S5. $[\Delta\sigma(H)/G_0]$-H results and Maekawa-Fukuyama fitting curves for x=0.42, thickness=30 nm sample at 2 K, 5 K, 10 K and 12 K.

According to Fig. S5, the *[Δσ(H)/G$_0$]-H* relationship and Maekawa-Fukuyama fitting results are well fitted, thus allows for further analysis based on Maekawa-Fukuyama expression.

Relative fitting formulas

For R_s-T results in Fig. 2(b), we adopt Hamman model of Kondo effect for further analysis. The formula is shown as follows:

$$R_S(T) = R_0 + AT^2 + BT^5 + R_K(T/T_K) \tag{S1}$$

Here, the R_0 is the residual resistance, the AT^2 describes the electron-electron scattering and BT^5 originates from electron-phonon interaction dependent resistance, while the last part is Kondo term, and can be expressed as follows:

$$R_K(T/T_K) = C(1 - \frac{ln(T/T_K)}{\sqrt{(ln(T/T_K))^2 + \pi^2(S(S+1))}}) \tag{S2}$$

Among the equation, C is a relative constant term, T_K means the effective Kondo temperature, and S is the effective spin of magnetic scattering center. As the fitting curves shows good consistency with R_s-T results in Fig. 2b, the variation of different fitting factors with respect to different samples are listed in Table S1.

Table S1. Fitting factors for R_s-T results of different NSAMO/STO samples shown in Fig. (2b) by using equation (S1) and (S2).

Sample	R_0 (Ω/□)	A (Ω/□K^2)	B (Ω/□K^5)	C (Ω/□)	T_K (K)	S (a.u.)

0.14, 20nm	2381.631	0.503	$6.599*10^{-8}$	924.822	12.224	0.090
0.14, 30nm	956.828	0.052	$1.964*10^{-9}$	298.081	70.516	0.063
0.28, 30nm	1861.064	0.615	$8.547*10^{-9}$	277.446	9.651	0.046
0.42, 30nm	655.408	0.212	$3.662*10^{-9}$	117.272	10.460	0.029

According to Table S1, the lattice disorder is enhanced in some aspects as the *A* and *B* order arrives a higher value, and the T_K tends to get smaller first as the x increases but will get relatively steady as the x continue to grow up.

For fitting of two types of carriers based on results in Fig. 4(a), we adopt a dual-channel carriers formula, which can be expressed as follows:

$$R_{xy} = \frac{H\left(n_1\mu_1^2 + n_2\mu_2^2\right) + H\left(\mu_1\mu_2 H\right)^2(n_1 + n_2)}{e(n_1\mu_1 + n_2\mu_2)^2 + e\left(\mu_1\mu_2 H\right)^2(n_1 + n_2)^2} \tag{S3}$$

$$R_S(0) = \frac{1}{e(n_1\mu_1 + n_2\mu_2)} \tag{S4}$$

Where n_1 and n_2 means the carrier density of different carriers, μ_1 and μ_2 represents corresponding mobility, and H is the magnetic field. Formula (S3) is restricted by Formula (S4).